

ELECTRONOTES

71

Newsletter of the Musical Engineering Group
203 Snyder Hill Road
Ithaca, N. Y. 14850

VOLUME 8, NUMBER 71

NOVEMBER 1976

GROUP ANNOUNCEMENTS:

CONTENTS OF EN#71

Page 1	News Items
Page 3	The Bandpass Filter Response and Electronic Music Applications -by Bernie Hutchins
Page 14	The ENS-76 Home-Built Synthesizer System - Part 5: -by Bernie Hutchins
Page 14	Introduction to the New VCF Designs
Page 15	ENS-76 Voltage-Controlled Filter - Option 1
Page 19	ENS-76 Voltage-Controlled Filter - Option 2
Page 22	Record Reviews: -by Craig Anderton

This newsletter is concerned mainly with filters. We start off with a study of the bandpass filter and analyze it from a mathematical and musical point of view. In particular, we develop some applications where the filter produces control signals. The filter has been used for years to produce complex patterns for "scope art" and it should be realized that these same patterns are useful as controls for musical parameters. Secondly, we are presenting the first two of the ENS-76 voltage-controlled filters. These came out a little earlier than we planned and since we found some very useful improvements, we decided to get them out right away. In particular, we have developed filters achieving high-Q at high frequency using a compensation technique that was available in the literature.

NEW MEMBERS AND CHANGES:

Edward A. Dudley	447 Blythwood Rd., Toronto, Ont. Canada M4N 1A8
Pierre FaFard	701 Duchesway, St-Justin, P. Quebec, Canada J0K 2V0
Bill Van Hassel	35 New Street, New Hope, PA 18938
David Kramlich	56 Bay State Rd #3, Boston, MA 02215
Robert Lange	105 Bingham, Rumson, NJ 07760
G. Oczkowski	6-703 Corydon Ave., Winnipeg, Manitoba, Canada R3M 0W4
Leonard Sasso	2983 Alexander Rd., Laguna Beach, CA 92651

NEWS ITEMS:

Copies of the proceedings of the Music Computation Conference II (Nov. 7-9, 1975) are available from: Proc. of the Music Computation Conference II, Continuing Education in Music, Univ. of Ill. at Urbana-Champaign, 608 S. Mathews, Urbana, IL 61801. Orders for these should be sent before Dec. 6, 1976. Available papers are:

- Part 1. Software Synthesis Techniques, Papers by Ferretti; Justice; Petersen; Saunders; Kaehler; Zuckerman & Steiglitz; and Cherubini. (75 pages - \$3.00)
- Part 2. Composition with Computers, Papers by Beckwith; Chadabe; Gressel; Howe; Rothenberg; and Tipei. (83 pages - \$3.00)

Part 3. Hardware for Computer-Controlled Sound Synthesis, Papers by Beauchamp, Pohlmann and Chapman; Gross; Kriz; Roy (59 pages - \$3.00)

Part 4. Information Processing Systems, Papers by Austin and Bryant; Charnasse; Dal Molin; Rosenboom; Peters (96 pages - \$4.00)

Make checks payable to the Univ. of Ill.

The following is a list of Audio Engineering Society Preprints from the Spring 1976 and Fall 1976 conventions that are of interest to engineers working with electronic music. These preprints can be obtained at a cost of \$2.00 each (\$1.50 each for AES members) and can be ordered from: Audio Engineering Society, 60 E. 42nd St., Room 449, New York, NY 10017.

Spring 1976 (Los Angeles)

- 1094 (D-2) Nyle A. Steiner, "An Electronic Valve Instrument (Trumpet) for Controlling an Electronic Music Synthesizer"
- 1101 (C-1) James G. Simes, "An Almost Locked Oscillator for Electronic Music Synthesis"
- 1102 (C-5) Philip West, "Use of Tape Recorders in Real-Time Electronic Music"
- 1104 (D-3) Tracy Lind Petersen, "Analysis-Synthesis As a Tool for Creating New Families of Sound"
- 1110 (D-6) Lee Ferguson, "A Polyphonic Music Synthesizer Utilizing Master Programmed Electronic Synthesis Modules for Each Key"
- 1121 (D-1) Thomas Wood, "A High-Speed Digital-to-Analog Conversion System for Digital Music Synthesis"
- 1123 (C-3) Brent Gabrielsen, "A Patchable Electronic Music Percussion Synthesizer"
- 1129 (C-2) Bob Moore "A 'Hybrid-Synthesizer' "
- 1133 (D-5) Patrick Gleeson, "Things Any Boy Can Do With a 16-Track, a DBX, and an EP Polyphonic Synthesizer"

Fall 1976 (New York City)

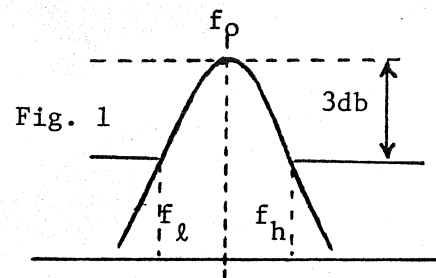
- 1142 (L-2) J. Stanley Kriz, "An Audio Analog-Digital-Analog Conversion System"
- 1146 (E-1) James A. Moorer, "The Use of the Phase Vocoder in Computer Music Applications"
- 1161 (E-2) James Michmerhuizen & Michael Gilbert, "A Digital Rhythm and Timing Generator for Electronic Music Applications"
- 1162 (B-4) C. J. Evans & J. Dawson, "A Feedforward Controlled Delay-Line Limiter"
- 1165 (D-5) Walter Jung, "Application Considerations for IC Data Converters Useful in Audio Signal Processing"
- 1166 (E-5) Gene P. Weckler, "Making Music with Charge-Transfer Devices"
- 1166 (F-4) Gene P. Weckler, "Signal Processing with Charge-Transfer Devices"
- 1172 (E-3) Thomas Oberheim, "A Programmer for Voltage-Controlled Synthesizers"
- 1185 (H-6) Eero Leinonen, Matti Otala, & John Curl, "Method for Measuring Transient Intermodulation Distortion (TIM)"
- 1190 (L-1) Francis F. Lee & David Lipschutz, "Floating Point Encoding for Transcription of High Fidelity Audio Signals"
- 1191 (L-6) Peter W. Mitchell & Richard E. DeFreitas, "A New Digital Time-Delay and Reverberation System, Part II: Psychoacoustics vs. Practical Electronics"

A position with title Audio Engineer/Technician and Training Associate is open at the University of Miami. Interested persons should send credentials to: Ted J. Crager, School of Music, Univ. of Miami, Coral Gables, FL 33124. We have sent them copies of the forms we have on individuals who contacted Electronotes seeking employment in electronic music.

THE BANDPASS FILTER RESPONSE AND ELECTRONIC MUSIC APPLICATIONS:

-by Bernie Hutchins, ELECTRONOTES

A typical bandpass filter response is shown in Fig. 1. The principal parameters which characterize the bandpass response are the center frequency (the maximum response) and the "Q" of the filter which is a measure of the sharpness of the response. The Q of the filter is generally taken to be the center frequency divided by the 3db bandwidth $f_h - f_l$.



The voltage-controlled bandpass filter has an obvious function in electronic music in that it can filter a complex waveform and thus control the harmonic content that appears at the output. Other uses are of course possible. With a high Q and white noise at the input, the filter passes a narrow band of frequencies which serve to define a feeling for musical pitch. The sharper the response, the clearer the feeling for musical pitch at the output. The sharp response bandpass filter can also be made to "ring" by exciting it with an impulse and letting the energy thus inserted decay as it oscillates. These applications are suggested by figures 2a, 2b, and 2c.

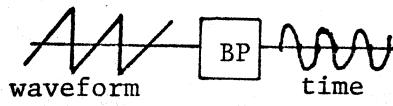


Fig. 2a

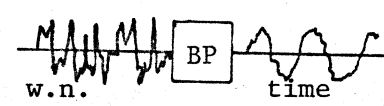


Fig. 2b

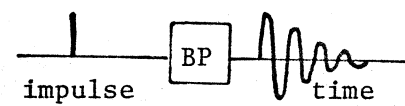
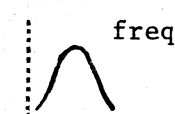
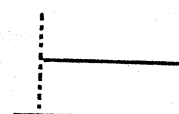
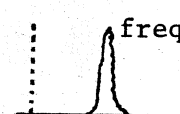
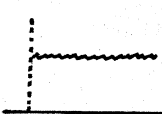
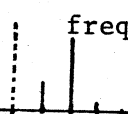
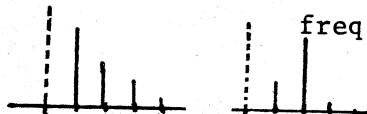


Fig. 2c



FREQUENCY RESPONSE

Although inductors are seldom used in audio filters these days, it is often useful to use them "on paper" to demonstrate certain principles which may not be so clear with active RC filters. A well known LC bandpass filter is shown in Fig. 3, and is probably familiar to readers who have studied radio frequency circuits where inductors are most certainly practical. We can easily derive the transfer function for the series RLC circuit in Fig. 3 by just considering it to be a voltage divider, and using the complex (Laplace) frequency variable "s". By inspection we have:

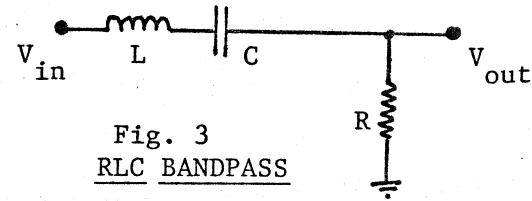


Fig. 3
RLC BANDPASS

$$T(s) = \frac{V_{out}}{V_{in}} = \frac{R}{R + sL + (1/sC)} \quad (1)$$

Clearly we are interested in the "resonant" case where $sL = -(1/sC)$ in which case $T(s)$ becomes $R/R = 1$, its maximum value. This happens for a particular value of s which we shall denote s_0 . Thus, $s_0^2 = -1/LC$, and we can let s_0 take on the value $j\omega_0$ and we then arrive at $\omega_0 = 1/\sqrt{LC}$. Next we note that nothing prevents us from multiplying the top and bottom of equation (1) by s/L and this gives:

$$T(s) = \frac{s(R/L)}{s^2 + s(R/L) + 1/LC} \quad (2)$$

This second form of equation (1) shows more clearly the fact that the denominator of $T(s)$ is really second order. Furthermore, we can identify the constant term in the denominator ($1/LC$) with the square of the center frequency (ω_0^2) and this will prove a useful reference point. We will then want to consider the coefficient of the s term in the denominator, and will find that it is this term which determines the sharpness (Q) of the bandpass response.

The approach we shall use to show the relationship of the coefficient of s and the Q of the filter will be to first assume the correct answer and then show that it all works out right. Thus, the general form of the bandpass response will be assumed to be:

$$T(s) = \frac{As}{s^2 + (\omega_0/Q)s + \omega_0^2} \quad A = \text{constant} \quad (3)$$

Note that for the moment we have not shown that the Q in equation (3) is the same as the Q described in the first paragraph of this report. We shall just note that since we propose that Q be dimensionless (since it is the ratio of frequencies), the constant ω_0 is needed to keep the denominator second order in the dimension of frequency. Thus what we have done in equation (3) is reasonable and will be justified by the final results.

Since we will be concerned here with the values of the frequency response that are down 3db from the peak, it will be necessary to determine the actual frequency response, not just the transfer function. To do this we evaluate T(s) for $s = j\omega$ and take the magnitude $|T(j\omega)| = [T(j\omega) \cdot T(-j\omega)]^{1/2}$. This is applied to equation (3) and we shall set $A=1$ for convenience.

$$|T(j\omega)| = \left[\frac{j\omega}{(j\omega)^2 + \frac{j\omega_0\omega}{Q} + \omega_0^2} \cdot \frac{-j\omega}{(-j\omega)^2 - \frac{j\omega_0\omega}{Q} + \omega_0^2} \right]^{1/2} \quad (4a)$$

$$= \left[\frac{\omega^2}{(\omega_0^2 - \omega^2 + \frac{j\omega_0\omega}{Q}) \cdot (\omega_0^2 - \omega^2 - \frac{j\omega_0\omega}{Q})} \right]^{1/2} \quad (4b)$$

$$= \left[\frac{\omega^2}{(\omega_0^2 - \omega^2)^2 + \frac{\omega_0^2\omega^2}{Q^2}} \right]^{1/2} \quad (4c)$$

$$= \left[\frac{Q^2/\omega_0^2}{1 + Q^2 \frac{(\omega_0^2 - \omega^2)^2}{\omega_0^2\omega^2}} \right]^{1/2} \quad (4d)$$

$$= \left[\frac{Q^2/\omega_0^2}{1 + Q^2 \left[\frac{\omega}{\omega_0} - \frac{\omega_0}{\omega} \right]^2} \right]^{1/2} \quad (4e)$$

The final result (4e) may seem a little awkward at first, but it is in a form that will be very useful to us. For example, we can see directly from this that when $\omega = \omega_0$, the frequency response is a maximum since only a one is in the denominator. Secondly, when we go to look at the 3db points (half power points), we will just want to see how a denominator of 2 will occur, and this is a matter of setting the second term in the denominator equal to one.

By consulting Fig. 1, we see that the frequency f_0 is a unique point in that it is the only value of frequency that has no other frequency value giving the same response. All others have two frequencies for a given value of response, and one of these is below f_0 and the other is above. We will want to use equation (4e) to find a relationship between such points. It will be convenient to use radial frequencies corresponding to the notation of equation (4e). We could use any value of response in what follows, but it will be most direct if we choose the frequencies where the response is down 3db from the peak value. The lower frequency is ω_L , the center is ω_0 , and the upper one is ω_h . It is then clear from equation (4e) that the 3db points are related by:

$$\frac{\omega_l}{\omega_0} - \frac{\omega_0}{\omega_l} = \frac{\omega_h}{\omega_0} - \frac{\omega_0}{\omega_h} \quad (5)$$

This is easily solved to give:

$$\omega_l \omega_h = \omega_0^2 \quad (6)$$

Equation (6) is quite interesting. It says that the center frequency is the geometric mean of the upper and lower 3db frequencies (and in fact, of any two frequencies having the same response value). This is a very convenient way of finding the actual center frequency of some low Q bandpass filters which have a broad top as it may be difficult to locate the maximum response of such filters. Also note that the center frequency is not the average of these values, although this is an excellent approximation for high Q, and is often used for high Q cases. However, for low Q, be sure to determine the center frequency as the square root of the product.

Next we want to determine the 3db bandwidth $\omega_h - \omega_l$, which will be denoted by B. Using equation (6) we get:

$$B = [\omega_h - \omega_l] = \left[\omega_h - \frac{\omega_0^2}{\omega_h} \right] = \left[\frac{\omega_0^2}{\omega_l} - \omega_l \right] \quad (7)$$

We then select one of the 3db frequencies (ω_h) and arrive at the expression:

$$B = \omega_0 \left[\frac{\omega_h}{\omega_0} - \frac{\omega_0}{\omega_h} \right] \quad (8)$$

From equation (8) we can arrive at the expression:

$$\left[\frac{\omega_h}{\omega_0} - \frac{\omega_0}{\omega_h} \right]^2 = \frac{B^2}{\omega_0^2} \quad (9)$$

We can now complete the task by observing that for 3db down, the frequency response $|T(j\omega)|$ should be down by $\sqrt{2}$ and thus the denominator in the brackets in equation (4e) should be 2, and thus:

$$Q^2 \left[\frac{\omega_3}{\omega_0} - \frac{\omega_0}{\omega_3} \right]^2 = 1 \quad (10)$$

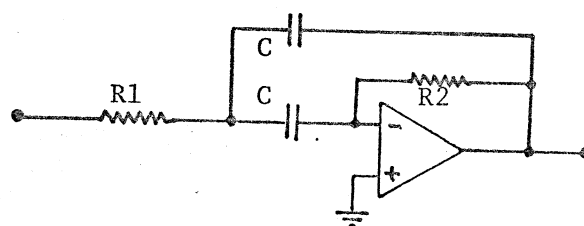
where ω_3 is one of the 3db frequencies, for which we can use ω_h . Substituting into equation (10) from equation (9) gives $Q^2 B^2 / \omega_0^2 = 1$ or:

$$Q = \omega_0 / B = \omega_0 / (\omega_h - \omega_l) = f_o / (f_h - f_l) \quad (11)$$

Thus equation (11) verifies equation (3) and the information on Fig. 1.

The importance of the above calculations is that we can now pull the most important of the bandpass parameters (f_o and Q) directly from the transfer function of the network by cross-matching against equation (3). For example, the transfer function of the RLC series circuit can be used and it can be shown that $Q = (1/R)\sqrt{L/C}$. As a second example, consider the well known bandpass RC active filter of Fig. 4.

Fig. 4
ACTIVE BANDPASS



It is not our purpose here to show how transfer functions are derived, so we will just give the transfer function of the network of Fig. 4 as:

$$T(s) = \frac{-s/R_1C}{s^2 + 2s/R_2C + 1/R_1R_2C^2} \quad (12)$$

From this we can easily get the center frequency and Q by comparing with equation (3).

$$\omega_0 = 1/C\sqrt{R_1R_2} \quad Q = (\sqrt{R_2/R_1})/2 \quad (13,14)$$

The above filter is fine as a fixed filter where great precision is not needed. There are however other active filter configurations that give better bandpass response at higher values of Q. These can be found in books on active filters. We want to look here at two more examples, but instead of following up on the circuit of Fig. 4, we will be looking at the state-variable filter, and the "biquad" circuit as these are the types of networks we will be using in voltage-controlled filters. There are several forms of the state-variable filter which are in common use. The calculations for some of these are a little complicated because it is generally easiest to use the standard inverting integrator. In voltage-controlled filters using the CA3080 however, it is quite easy to make a non-inverting integrator, so we can then get the required negative feedback by summing into the simple inverting summer. The basic structure thus reduces to that shown in Fig. 5.

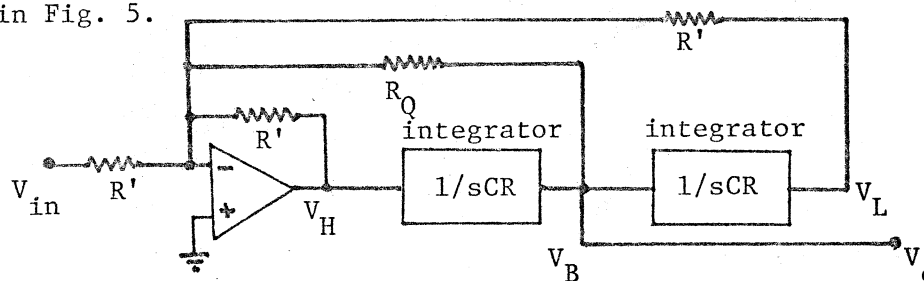


Fig. 5 STATE-VARIABLE FILTER

$$T(s) = \frac{-s/RC}{s^2 + \frac{R'/R_Q}{RC}s + \frac{1}{R^2C^2}}$$

From this, it is clear by comparing with equation (3) that $\omega_0 = 1/RC$ and $Q = R_Q/R'$ which is a simple and easy to remember result. Note in particular that both ω_0 and Q can be set simply and independently. This is a nice thing to have in a voltage-controlled filter for electronic music.

The structure of the "Biquad" is shown in Fig. 6. This filter has a bandpass and a low-pass output. Note that it is different from the state variable.

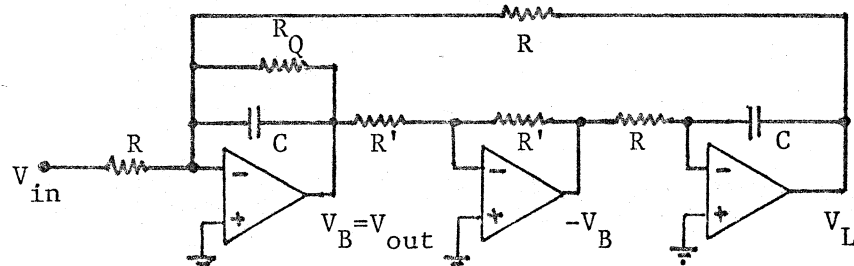


Fig. 6 BIQUAD ACTIVE FILTER

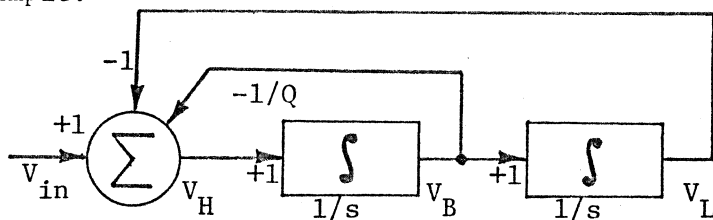
$$T(s) = \frac{-s/RC}{s^2 + (1/R_Q)s + 1/R^2C^2}$$

From the transfer function, we note by comparing with equation (3) that $\omega_0 = 1/RC$ and $Q = R_Q/R$. Here we see that the Q is set by the ratio of one independent resistor (R_Q) and one resistor (R) which is a frequency determining resistor. In fact, it is clear that the Q and ω_0 rise together as R decreases. The reader can easily see that this means that the filter has a constant bandwidth. That is, if the bandwidth is 50 Hz for a center frequency of 100 Hz, the Q is 2. Now, by decreasing R, we would eventually arrive at a point where the center frequency is 1000 Hz. If Q were constant, the bandwidth would be 500 Hz. But the Q has gone up by a factor of 10 and is now 20, and the bandwidth is still 50 Hz. Generally, the musical value of such (constant bandwidth) filters is not great as constant Q filters. But, there is one thing to note. We will see soon that a constant bandwidth filter has a constant ring time, unlike the constant Q filter which rings longer at lower frequencies. We shall want to take a careful look at this later, and we should also note that with voltage-controlled Q, we may be able to get constant bandwidth with the state variable filter as well.

While on the subject of voltage-controlled filters, it should be noted that there are at least two ways to insert a signal into a state-variable VCF. The first way is basically as shown in Fig. 5. The second way provides a "Limit" input through a voltage-controlled Q section and has been used by Terry Mikulic in his filter in EN#34, page 17. Below in Fig. 7a and Fig. 7b we show the two methods where we have taken $RC=1$ to keep things simple.

Fig. 7a

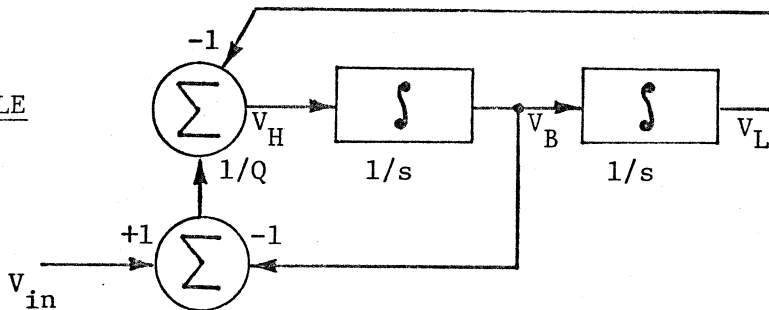
STATE VARIABLE
STANDARD INPUT



$$T(s) = \frac{V_L}{V_{in}} = \frac{s}{s^2 + (1/Q)s + 1}$$

Fig. 7b

STATE VARIABLE
LIMIT INPUT



$$T(s) = \frac{V_L}{V_{in}} = \frac{s/Q}{s^2 + (1/Q)s + 1}$$

The reader should note that the only difference between the two is while V_{in} is fed in through a +1 path in Fig. 7a, it is fed in through a $+1/Q$ path in Fig. 7b. Thus, all that we have really accomplished is an attenuation of the input by a factor of $1/Q$, and this carries through to the transfer functions $T(s)$ as can be seen. We could convert 7a to 7b by just changing the +1 path to $+1/Q$ and not use the second summer, but the second summer shown in Fig. 7b is what we find in practical voltage-controlled Q setups, and it is certain that the factor $1/Q$ is the same for both the input and the V_B feedback in the case of Fig. 7b. The advantage of the limit input should be clear from a study of the transfer functions. In the case of 7b, the peak of the bandpass (and of the other outputs when used) is a constant as Q changes. This keeps the filter from saturating when high Q is achieved, as the input voltage level is cut back when the Q goes up. For fixed Q , there is probably no reason to choose one structure over the other if one just judges by the output sounds produced. When voltage-controlled Q is used, it is a different story. When the regular input is used, the output amplitude level will increase with Q , and the passband of course sharpens with increased Q . With the limit input, only the sharpening of the passband occurs. Probably a filter with voltage-controlled Q should have both types of input available.

TIME RESPONSE

At this point in our analysis, we want to take a look at the bandpass from the point of view of its time response. Here is where we want to see exactly what happens when we "ring" the bandpass filter. The first thing we want to do is to take the standard bandpass transfer function and factor its denominator (using the quadratic formula):

$$T(s) = \frac{As}{s^2 + (\omega_0/Q)s + \omega_0^2} = \frac{As}{(s + \alpha + j\omega_d)(s + \alpha - j\omega_d)} \quad (15)$$

where $\alpha = (\omega_0/2Q)$ and $\omega_d = \omega_0\sqrt{1 - 1/4Q^2}$ as can be easily verified by substituting back. We are interested in the case where the denominator becomes zero (and hence, $T(s)$ blows up). These are clearly values s_1 and s_2 such that $s_1 = -\alpha + j\omega_d$ and $s_2 = -\alpha - j\omega_d$. These values are called the "poles" of the transfer function. Note that the two poles have a real part (α) and an imaginary part (ω_d). Thus we have to represent them as points in the complex "s-Plane" where s is the complex Laplace variable we have been

finding useful. A plot of these pole positions is shown in Fig. 8. The s-Plane is laid out in terms of a real axis (σ) and an imaginary axis ($j\omega$). More information on the s-Plane can be found by reading the article on low-pass filters in EN#41, reprinted in Chapter 5d of the Musical Engineer's Handbook. For the moment, we will just note that we are interested in the value of a function (such as $T(s)$) of a complex variable (s) and since the variable is complex ($s = \sigma + j\omega$), we must represent its value as the elevation of a surface above a plane (the s-Plane). The poles thus represent infinitely high points above the plane. The portion of the surface around them is thus expected to be very high. Note also that the point $s = 0$ causes the numerator of $T(s)$ to be zero, so this point is called a "zero" of $T(s)$. In between these poles and zeros, we have a curved surface. Points of equal elevation on the surface form flat contours, and these loop around the poles and connect up. We thus can plot contours such as the 3db (half power) contour as shown in Fig. 9. For frequency response, we were interested on the value of the transfer function above the $j\omega$ -axis going from 0 to ∞ . We can see that for $s = 0$, $T(s) = 0$ as well. Moving upward along the $j\omega$ -axis, we move to higher ground. When we reach $\omega = \omega_d$, we are near the highest point, but the zero at $s=0$ has in effect lowered the ground at ω_d and the actual peak is not reached until we reach ω_0 . Beyond ω_0 , it is downhill all the way to $\omega = j\infty$.

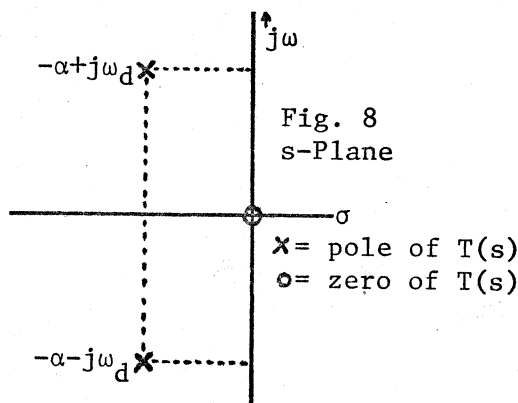


Fig. 8
s-Plane

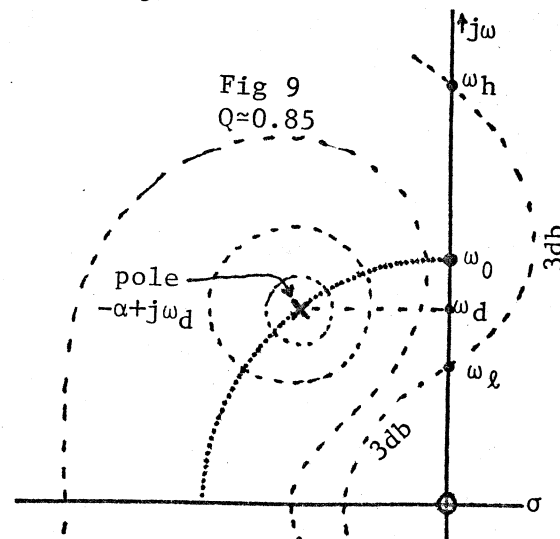


Fig 9
 $Q \approx 0.85$

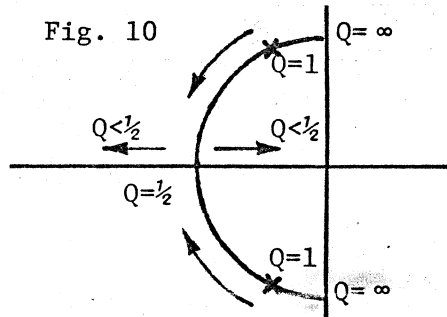


Fig. 10

We have now had two looks at the way things are placed around the s-Plane, and should have some idea about it even if we don't know all the details. We want to take one more look at it, as seen in Fig. 10 where we see how the poles move as Q changes. We saw in Fig. 8 that the poles were placed according to the values of a and ω_d , and we obtained these two parameters as a function of Q only. Thus, we can plot a "locus" of points showing how the poles move as Q changes. Here we show mainly Q from infinity down to $1/2$, as these are the only cases where the poles are complex (the $Q = 1/2$ case being the critically damped "Gaussian" filter case.) Before considering filter ringing, note that the peak of the frequency response remains at ω_0 in all cases even though the pole frequency ω_d changes with Q . This is because the zero at $s=0$ has pulled down the surface along the $j\omega$ -axis across from ω_d as we have described above.

In order to understand filter ringing, we have to study the impulse response of a filter, but first we have to see what is really meant by $T(s)$. We have written $T(s) = V_{out}/V_{in}$ and we are also accustomed to measuring frequency response using sine waves, so we might think that V_{out} and V_{in} are functions of time. Well, they are functions of time, but we can't write a function of one variable equal to a function of another variable so what is meant by $T(s)$ must be:

$$T(s) = V_{out}(s)/V_{in}(s) \quad (16)$$

where $V_{out}(s)$ and $V_{in}(s)$ are the Laplace transforms of their time waveforms. [The reader should take a moment to consider why it is that we can actually measure $T(s)$ in terms of sinusoidal waveforms which vary in time.] The meaning of this is that $T(s)$ is a function

that we can use to get the Laplace transform of the output if we know the Laplace transform of the input. We want to ring the filter, and this takes a sharp spike waveform or impulse. Mathematically, the ideal spike is the delta function $\delta(t)$ and the Laplace transform of $\delta(t)$ is just 1. The reader will probably find this to be probable (believable) if he considers that the Laplace representation is a form of frequency representation (spectrum), and he probably already knows that a sharp spike sounds like a "click" which is wideband noise, or a flat, constant spectrum, which can be taken to be one. We can thus do the following:

$$T(s) = V_{out}(s)/V_{in}(s) \quad \text{or:} \quad V_{out}(s) = T(s) \cdot V_{in}(s) \quad (17a, b)$$

$$\text{for } V_{in}(t) = \text{impulse} = \delta(t), V_{in}(s) = 1 \quad (18a, b)$$

$$\text{Thus: } V_{out}(s)_{\text{impulse}} = T(s) \cdot 1 = T(s) \quad (19)$$

Taking inverse Laplace transforms:

$$V_{out}(t)_{\text{impulse}} = L^{-1}[T(s)] = h(t) \quad (20)$$

where the symbol L indicates the Laplace transform (L^{-1} is thus the inverse transform). Equation (20) thus gives us the important result that the impulse response (in time) is just the inverse Laplace transform of the transfer function $T(s)$. We already have $T(s)$. Thus to find how the filter responds to an impulse, we just have to look up the Laplace transform pairs in the tables. One such pair is shown below:

$$\begin{array}{ccc} \frac{s}{(s - a)(s - b)} & \xrightarrow{L^{-1}} & \frac{be^{bt} - ae^{at}}{b - a} \\ & \xleftarrow{L} & \end{array} \quad (21)$$

This is clearly of the same form as equation (15) for the bandpass filter. We could now plug into the inverse Laplace transform to get the time waveform of the ringing filter. However, the complete solution tends to obscure the important features rather than enhance them. Instead, we will just note that terms like

$$e^{(-\alpha - j\omega_d)t} = e^{-\alpha t} e^{-j\omega_d t} \quad (22)$$

will appear. This is a decaying exponential ($e^{-\alpha t}$) which controls the amplitude of a sinusoidal term ($e^{-j\omega_d t}$). Thus, we can justify to some extent our intuitive notion that the ringing filter produces a decaying exponential sinusoidal waveform. This waveform is shown in Fig. 11. We note further that the exponential decays with a time constant $1/\alpha = 2Q/\omega_0$. This is no surprise since we expect longer decay times as we increase the Q of the filter. What is more of a surprise is that the sinusoidal frequency is ω_d and not ω_0 as we might have expected. We can see however from Figures 8, 9, and 10 that for high Q , there is very little difference between ω_d and ω_0 .

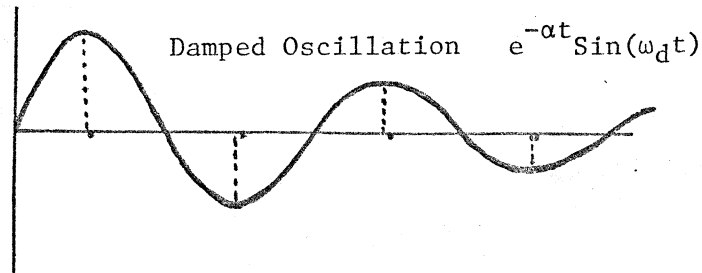


Fig. 11

An important formula on filter ringing is obtained by finding the amount of time it takes for the amplitude to die out to $1/e$ of its original value. This is just a matter of setting $e^{-\alpha t} = e^{-1}$ and hence $T_{ring} = 1/\alpha = 2Q/\omega_0$ which can also be written:

$$T_{ring} = \frac{Q}{\pi f_0} \quad (23)$$

There are several important things to notice about equation (22). First, it is a convenient way to measure Q in cases where the bandwidth is very small (thus for high Q)

and where it would be difficult to separate the 3db points. Thus Q can be measured by ringing the filter and finding the time constant of the decay envelope.

Secondly, note that for fixed Q, the ring time gets shorter as frequency rises. This is an important musical result, although it is not possible to say ahead of time if it is particularly useful or if it is a drawback. On the one hand, we know that many acoustic musical instruments have faster decay at higher pitches (the piano for example). On the other hand, we may want to use the ringing filter as a self-enveloping system where we would otherwise use an envelope generator (fixed time constants) and a VCO. In this case, the shorter decay times at higher frequency that would result from the ringing filter would be a drawback. However, we can have both results if we wish by using voltage-controlled Q. This is a good case for suggesting that Q should double for each one volt change of control. This would allow us to set up either constant number of decay cycles (fixed Q) or constant decay time (using voltage-controlled Q). These setups are shown in Fig. 12a and Fig. 12b. Note that a constant number of cycles for 12a is implied by equation (23) since $T_{ring} \cdot f_0 = \text{number of cycles} = \pi Q$, which is a constant for a constant Q.

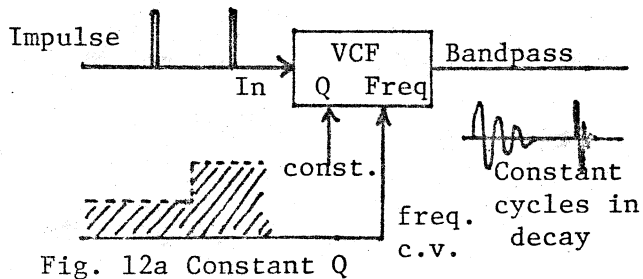


Fig. 12a Constant Q

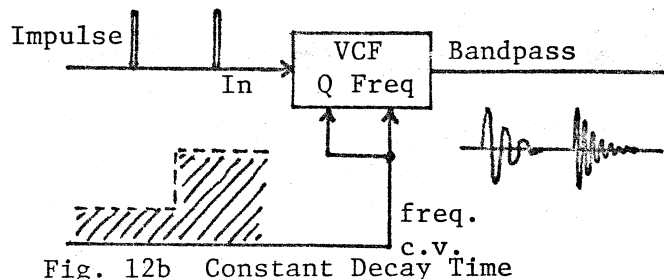


Fig. 12b Constant Decay Time

We now turn our attention to the question of the detuning from ω_0 to ω_d where

$$\omega_d = \omega_0 \sqrt{1 - 1/4Q^2} \quad (24)$$

This detuning for different values of Q is shown in Fig. 13.

<u>Q</u>	<u>ω_d/ω_0</u>	<u>Ring Cycles (1/e)</u>	<u>Ring Cycles (1/e⁶)</u>
0.5	0	0.16	0.95
0.6	0.55	0.19	1.15
0.7	0.70	0.22	1.34
0.8	0.78	0.25	1.53
1.0	0.87	0.32	1.91
1.5	0.94	0.48	2.86
2.0	0.97	0.64	3.82
3.0	0.986	0.95	5.73
4.0	0.992	1.27	7.64
6.0	0.997	1.91	11.5
10.0	0.9987	3.18	19.1
50.0	0.9995	15.9	95.5
100.0	0.999987	31.8	191

FIG. 13

TABLE OF DETUNING

VALUES DUE TO

DAMPING OF FILTER

[Ring cycles down
to 1/e⁶ is
approximately to
expected audible
range.]

From the table above, we can make one preliminary conclusion. For a detuning value which we might expect to notice (say 1%), we would have a Q of about 4, and a total number of audible cycles of only about seven. This may not be enough for the ear to detect a proper feeling for pitch. A study of similar cases causes one to conclude that it may not be possible to detect this detuning by ear - hence its musical importance is very small.

Before we discuss some additional applications of bandpass filters, we should say a few additional words on what we have discovered so far. First note that equation (22) is really a damped sinusoidal of some form. Thus, we can look at the damped oscillation as shown in Fig. 11 as being of the form:

$$e^{-\alpha t} \sin(\omega_d t) \quad (25)$$

The zero crossings of this waveform are clearly at times where $\sin(\omega_d t) = 0$, which is just what we expect from a sinusoidal. However, the individual lobes between the zero crossings are not sinusoidal lobes. You could prove this by differentiating equation (25) and setting the derivative equal to zero. It will serve here however to just note that the maximum and minimum points of the waveform fall at points in time that occur before the midpoints between zero crossings. For example, the maximum point of the first lobe will occur when the rate of change of the upward sinusoidal is equal to the rate of change of the downward exponential. Clearly this is before the normal peaking point of the sine wave (which occurs at the midpoint between zero crossings), because at the normal maximum of $\sin(\omega_d t)$, the combined waveform of equation (25) is moving downward because of the exponential damping factor. Now, beyond the maximum point of the waveform in equation (25), the exponential damping factor forces the sinusoidal down a little faster than normal, which tends to flatten the normally more rounded portion. Yet, the exponential damping works only on the amplitude of the sinusoidal (one in this case) and not on the waveform directly, so it is still necessary for the function $\sin(\omega_d t)$ to go to zero in order to get the zeros of the composite waveform of equation (25).

We have suggested above that the detuning from ω_0 to ω_d [Equation (24)] is not likely to be detected by ear since in cases where there is enough pitch shift, there are too few cycles in the decay. The detuning may be more important at low frequencies (say 1 Hz.) Even though the waveform is not directly audible in such cases, these low frequency detunings may be detectable indirectly, as when they are used as control signals. It is just this sort of use of the filter output as a control signal that we want to discuss in the suggested applications below. Also, in cases where the filter output is used to modulate another process, there may be a great difference between a modulating frequency that is exactly harmonically related to another frequency, and one which is only close.

There is another fine point which we are not able to completely rationalize here. Perhaps some reader can provide us with the answer. First, we note that when we measure the frequency response of the bandpass, the peak is always at ω_0 . Secondly, when we ring the filter, it oscillates (exponentially damped) at a somewhat lower frequency ω_d . All this is fine, but we now want to inquire about the response of the filter to a white noise input (flat spectrum). Since the input spectrum is flat in this case, we expect the output spectrum to have a peak at the maximum response point of the frequency response curve (which is ω_0). In another view, we can consider white noise to be a series of impulses of random amplitude and random time of occurrence. In this view, the response of the filter is the superposition of the individual impulse responses, each of which is an exponentially damped sinusoid with zero crossings corresponding to ω_d . For practical purposes, thus probably makes no difference at all, but it would be interesting to know if these two views do lead to the same result.

APPLICATIONS

We are very much accustomed to listening to the output signals from filters rather than using them as a control for some other processing unit. The three primary applications in Figures 2a, 2b, and 2c are examples where we listen to the output. The signals from filters are of course usable as controls. An example of such a case is shown in Fig. 14 where white noise is bandpass filtered at a frequency of about 7 Hz with moderate to high Q (say about 100). The resulting signal is a useful vibrato signal which can be applied to a VCO as shown. Experiments with this show that this is quite different from vibrato produced with a steady state waveform. For one thing, the depth changes somewhat randomly with a time constant on the order of a second or two. Thus, it sort of fades

in and out during an extended tone (and it is usually extended tones which employ vibrato). Another thing is that one can perceive the random nature of the process as some sort of subjective randomness in the output of the VCO. This is not to say that the resulting vibrato is more musical, or more natural, but just that it does have an interesting property. Some persons would perhaps describe it as a "spooky" vibrato as opposed to a "mechanical" vibrato from an oscillator control, and a "warm" vibrato which one would hear from a singer, for example.

The value of frequency modulation (FM) and dynamic depth FM has been demonstrated both theoretically and through its use in musical compositions. A typical patch for FM is shown in Fig. 15a, for dynamic depth in 15b, and for modulation by the ringing bandpass filter in 15c.

Fig. 14

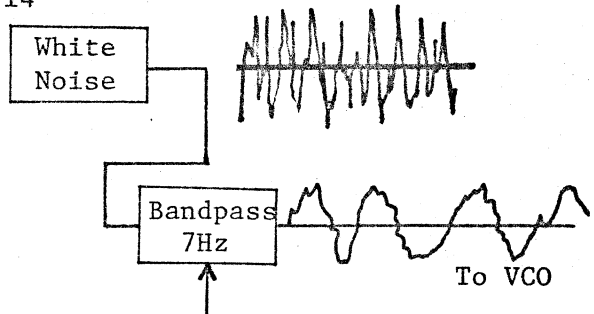


Fig. 15a

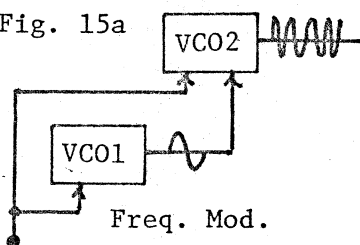


Fig. 15b Dynamic-Depth Freq. Modulation

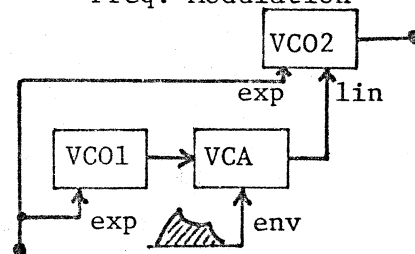
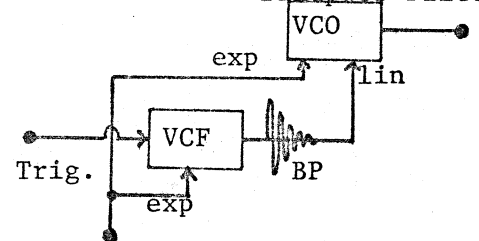
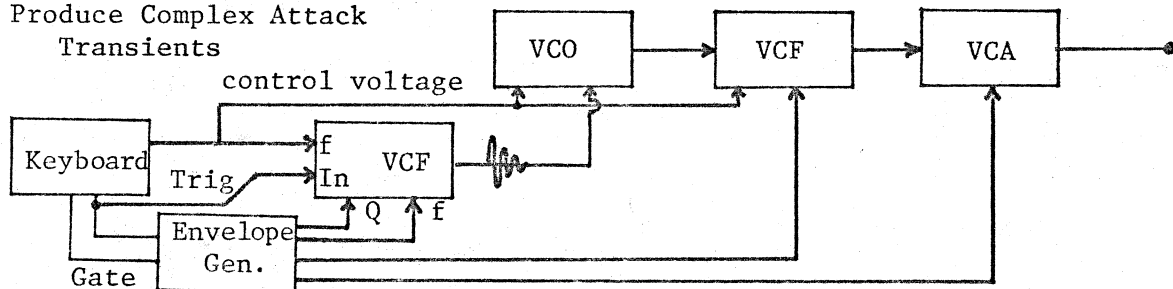


Fig. 15c FM by Ringing Bandpass Filter



The patch of Fig. 15a is standard, that of Fig. 15b is being explored (very useful for percussion effects), and that of 15c is relatively unknown as far as we can tell. Linear frequency modulation by a ringing bandpass filter is however a very useful way of producing very interesting musical transients (usually attacks). We had an envelope generator which did this back in EN#9, but it was not much used. As shown in Fig. 15c, the bandpass is rung by the trigger from the keyboard. This damped exponential sinusoid goes into the linear FM input of a VCO. It is well established that many musical instruments produce very strange effects during the initial part of their tones. This attack phase may have many frequency components which do not exist during the steady state that follows. The bandpass filter rung by the trigger produces a useful waveform for adding features during attack. Immediately after the trigger arrives, the output of the bandpass is at a maximum (producing the deepest FM and thus the widest distribution of sidebands). As the bandpass response decays, the modulation depth decreases, and this means there is less and less energy in the sidebands, and more and more in the central frequencies. A more complete patch for this method is shown in Fig. 16.

Fig. 16 Use of Ringing Bandpass To Produce Complex Attack Transients



Of course, you can also use the filter at very low frequency (1 Hz for example) and at high Q to produce a control signal that lasts several minutes, and yet still does decay uniformly. In another variation, a finite width pulse can be used (meaning, one which has a duration longer than the time constants of the filter input stages). For example, the pulse of Fig. 17 will cause a complex ringing in that the filter will start to ring and decay on the positive going edge, and then will be restarted by the negative edge. This complex transient is useful, and can be easily demonstrated by ringing the filter

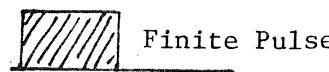
with a pulse from a VCO and altering the pulse width. This can be used as a control signal for FM as in Fig. 16, or as a timbre producing element by directly listening to the output of the filter. In this latter case, the frequency of the filter would probably be in the upper audio range while the pulse ringing it would be in the lower audio range.

While we have been discussing here mostly bandpass filters, the same generally applies to high Q low-pass and high-pass filters which can also be rung. There may be some obvious differences however. For example, with the high-Q low-pass rung by a square wave, the DC term will come through (that is, the two levels of the square wave will be passed through). This is illustrated in Fig. 18. It is easy to think of patches where this sort of waveform could give interesting results since it is basically two levels with starting transients.

SUMMARY

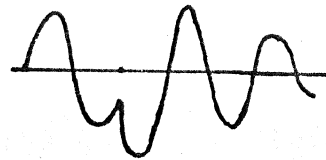
Since the mathematics above may have obscured much of the useful information for some readers, we will provide a brief summary of the important results as far as musical applications are concerned.

1. The "Q" of a bandpass filter is obtained as discussed in the first paragraph.
2. Once a transfer function is obtained, the center frequency and Q can be easily obtained by comparing with equation (3).
3. A state-variable filter provides constant Q while a Biquad provides constant bandwidth. When ringing the bandpass, constant Q means a constant number of cycles during decay (shorter ring times at higher frequency), while constant bandwidth means a ring time independent of frequency. Constant bandwidth can be obtained with a state-variable by increasing Q with the frequency.
4. A "Limit" input for a state variable filter is often provided along with voltage-controlled Q. This input supplies less signal to the filter as the Q is increased.
5. A filter which is rung provides an exponentially damped sinusoidal waveform (Fig. 11) (Equation 25). The frequency of this ringing is slightly below the center frequency of the filter, but probably this detuning is not detectable by ear.
6. The relation between Q, center frequency, and ring time to $1/e = 37\%$ is given by equation (23). This equation should be carefully studied.
7. There are numerous applications of bandpass filters and other VCF's which use the output of the filter as a control signal rather than using the output signal as an audible sound. These include vibrato, linear FM, and a number of schemes for generating complex transients.
8. There is a need for additional analysis and/or experimental measurements on the output of bandpass filters excited by impulses and with white noise. In particular, it would be useful to know the exact mathematical properties of such outputs, and correlate this information with data on aural perception to get a better idea of musical implications. For example, Metzger [J. Acoustic Soc. Amer., Vol. 42, No. 4, 1967, pg 896] shows that the peak of the Fourier Transform of equation (25) is actually below ω_d .



Finite Pulse

Fig. 17



Complex
Transient

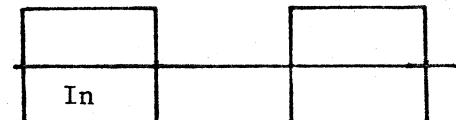
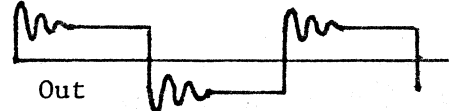


Fig. 18 Low-Pass Ringing



THE ENS-76 HOME BUILT SYNTHESIZER SYSTEM - PART 5:

-by Bernie Hutchins

In this installment, we will be giving two of the VCF designs for the ENS-76 series. The first of these is a new formulation of the state-variable filter, and has been made as simple as possible. The second filter is a revision of the filter given in EN#37. We expect to give two more filters in the future. One of these to come will have a cascaded state-variable configuration for 24db slopes, and the other will have a voltage-variable slope. The reader should keep in mind that many of the features in these filters are "interchangeable" in the sense that they may be used in structures other than the one they are actually presented in. The reader should feel free to select features from the different options to arrive at exactly the filter he needs.

INTRODUCTION TO THE NEW VCF DESIGNS

The VCF designs we will be using are all state-variable. We have found that this filter can not be improved upon either as a general purpose filter or as a special purpose one. We have changed around a few structures here and there in previous designs, and used a few new parts, but basically there is one major improvement which we have implemented, and this is the control of the runaway Q at high frequency.

We should point out right away that the compensation technique for controlling Q which we give here is not original with us. Actually, we discovered it in a recent paper [Sergio Franco, "Use Transconductance Amplifiers to Make Programmable Active Filters," Electronic Design, Sept. 13, 1976, pg. 98]. Ian Fritz pointed out to me that this same general technique was discussed by R. Sparkes and A. Sedra in "Programmable Active Filters," IEEE J. Solid State Circuits, Feb. 1973. This paper in turn leads us back to an earlier application of a similar technique to the biquad circuit in "The Biquad: Part I - Some Practical Design Considerations," by Lee Thomas, IEEE Trans. Circuit Theory, CT-18, May 1971 [Also reprinted in Active Inductorless Filters edited by S. K. Mitra, IEEE Press (1971)].

So what is it? Basically it is just a matter of adding in a couple of capacitors on the order of a few picofarads to produce a phase lead, compensating for phase shift at high frequency, thus stabilizing the filter at high Q and high frequency. Our previous VCF designs showed instabilities at high frequency and high Q. The circuit in EN#30 which used type 595 multipliers was very bad in this respect. It was found that the capacitor C9 in this case did stabilize the circuit. However, this design was then abandoned in favor of one using the CA3080 as a control element. The final result was the filter in EN#37. It turns out that it takes only a few picofarads to stabilize this filter. Since most stray capacitances are on this order, it is not too surprising that trouble with this filter did not appear for all builders, and certainly not for all builders at the same limiting points. None the less, it is a good idea to add in these capacitors or at least check to make sure that the response is not just marginally stable.

The basic structure of the state-variable filter is shown in Fig. 1. This should be familiar by now. It is a summer and two integrators, and the structure is stabilized by negative feedback from both integrators. As Q increases, the negative feedback from the first integrator decreases. Thus, higher Q is associated with a system that is less stable than lower Q situations. There is another way that negative feedback can be reduced. This is indicated by considering a more realistic model of the state-variable as shown in Fig. 2. Here we show in addition to the summer and integrators, a stage which adds some phase lag. This is not something we have added to the circuitry, but something that was there all the time. It is due to phase shifts across the IC's which is due to capacitances between the elements inside the IC's. This phase shift increases with higher frequencies. As this phase shift increases, negative feedback is lost in favor of positive feedback. Clearly if the phase shift is 180° , it is all positive feedback. One solution to this problem is shown in Fig. 3 where a phase lead network has been added to the inputs of the integrators. We add this only to the integrators because they each include two IC's while the summer is only one IC. Also, it is really only necessary to make some correction, and

not to correct for every little detail of the phase response. In fact, there are probably several break points in the phase response of the integrators while the network shown to provide the phase lead only corrects for the largest of these, or perhaps just gives an average which takes care of the problem. An exact correction would require accurate modeling of all the active devices, which would be unnecessary for our purposes.

We should note that the value of the capacitor C_{qc} is just a few picofarads when the resistors shown are the standard 100k and 220 ohm attenuating resistors used on the inputs of CA3080's. A capacitance of say 3pf is difficult to work with. We found in working with the circuit of EN#37 that when we soldered jumpers of about 1 inch onto the 100k resistors (so that we could easily solder on capacitors) that the two jumpers of about 1" separated by about 1/4" made a substantial improvement to the stability. For this reason, we suggest using attenuators for the CA3080's of 10K and 22 ohms for these circuits. This means that the compensating capacitors can be ten times as large. We will see that with better quality op-amps, even this change means that the compensation may be only 10pf or so. But the important thing is that the scheme does work.

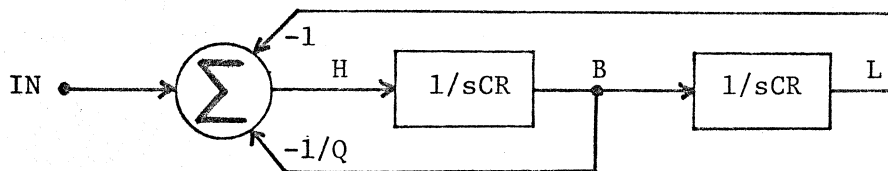


Fig. 1

BASIC STATE-VARIABLE

Fig. 2 STATE-VARIABLE WITH EXISTING PHASE SHIFTS

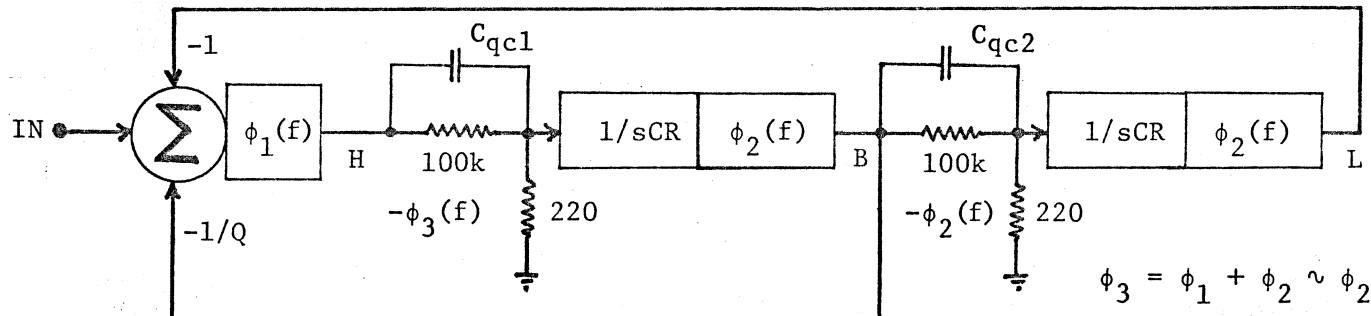
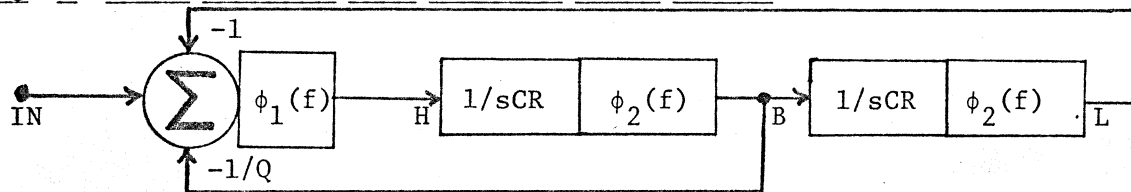


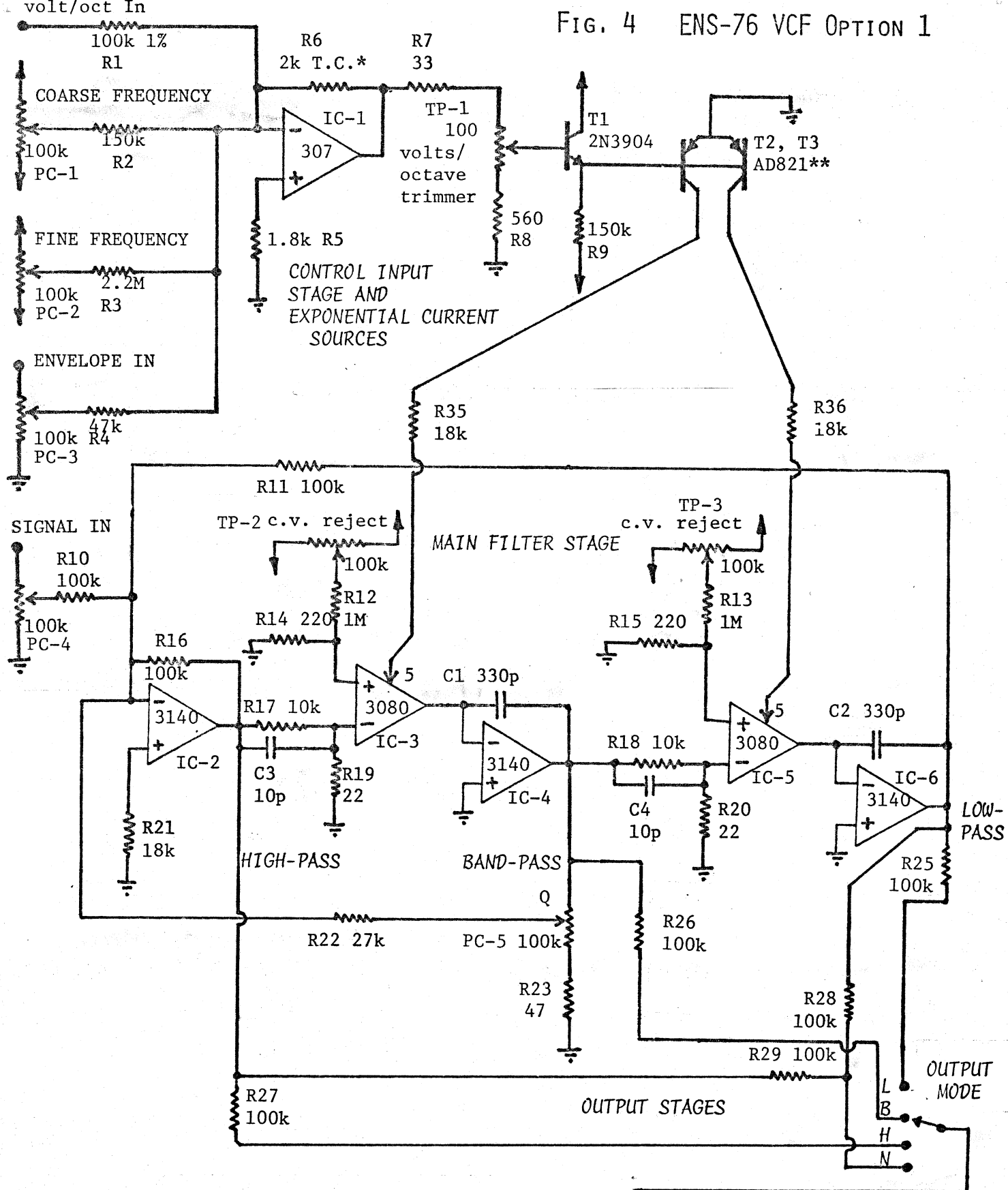
Fig. 3 STATE-VARIABLE WITH PHASE SHIFT COMPENSATION

ENS-76 VOLTAGE-CONTROLLED FILTER - OPTION 1

The first of the ENS-76 VCF options is shown on page 16. This filter features a state-variable structure giving second order responses for low-pass, band-pass, and high-pass. A manual control for Q is provided, and a notch output is also available. The filter has a range from below 1/10 Hz up to about 18 kHz, and Q is variable from about 1/4 to well over 500.

The circuitry of the filter is quite similar to what we have done before. There are about four changes which we should point out. First, there is a somewhat different exponential current source, which is a dual source. Secondly, we use the new RCA CA3140 for the filter op-amps because it seems to have a very small phase shift relative

FIG. 4 ENS-76 VCF OPTION 1



Bypass -15 with 33 mfd
+15 with 10 mfd

* ** See Text

to other op-amps we tried. Thirdly, phase-lead circuitry has been used to prevent Q-enhancement. Finally, we used a mode switch on the output instead of using separate output jacks for each of the modes. We will discuss these changes in more detail below.

The exponential current stage is really just the basic structure described by Terry Mikulic in EN#37. A standard summing network (IC-1) sums the control voltages and scales them to about 20mv change for a one volt change of the input control. This is trimmed to about 18mv by the 100 ohm trimmer TP-1. T1 is an emitter follower which sets the I_o current for the exponential converter ($I_o = 15/R9$) and also drives the converter transistor T2. A second transistor T3 is driven in parallel with T2 and thus provides an identical current (assuming the transistors T2 and T3 are matched). Resistor R6 is a 2k +3500ppm/ $^{\circ}$ C temperature compensating resistor (Tel Labs type Q81). For non-critical work, you can use a 2k 5% carbon resistor. Likewise, T2-T3 is specified as a matched pair (Analog Devices AD821) but for non-critical work, you can use a pair of 2N3906's glued together. These exponential currents are driven through resistors R35 and R36 into the control pins (pin 5) of the CA3080's. Since the collectors of T2 and T3 can reach no higher than about zero volts, the current into pin 5 of the CA3080's is limited to less than 15volts/18k = 0.83ma. The resistors R35 and R36 serve to limit this current, and thus limit the upper frequency of the filter to about 18 kHz, but otherwise have no effect on the circuit and can be ignored during analysis. In previous circuits, we have driven such a pair of resistors from a single exponential current source. For currents such that a substantial voltage is developed across these resistors the resistors tend to divide the current equally between the two CA3080's. However, for low currents, there is very little voltage drop across these resistors and the current may not be shared equally. Thus, the dual source in this example is probably a better idea.

In a number of lab tests, we found that the new RCA CA3140 was about an order of magnitude better than the LM307 when used in state-variable filters. This was determined when we were testing for Q-enhancement. Since we wanted a very high-Q filter, we decided to use the CA3140 here and deal with the fact that it is not a satisfactory output driver by using an output buffer (IC-7). The low bias current of the CA3140 also permits the filter to operate at very low frequency. We actually found that we could ring the filter as low as 0.002 Hz, but at that low a frequency, we did not have enough time to make any measurements of control accuracy. Thus, we are just claiming response down to 1/10 Hz as we have verified this.

Before going on to describe how the phase correction circuitry is adjusted, we should say a few words about how the filter frequency is controlled by the control current, how the Q is determined, and how the control voltage reject trim pots are adjusted. First we note that the basic equation for the CA3080 is:

$$I_{out} = 19.2 \cdot I_{ABC} \cdot V_{di}$$

where I_{ABC} is the control current into pin 5, and V_{di} is the differential input voltage (the actual voltage difference between pins 2 and 3 of the CA3080). Since there is an attenuator of 10,000:22 on the input, and the (+) terminal is effectively zeroed, the input voltage (V_{in}) is related to V_{di} by $V_{in} = 456 \cdot V_{di}$. Substituting this back into the basic CA3080 equation, we get:

$$R_{eq} = V_{in}/I_{out} = 23.7/I_{ABC}$$

where R_{eq} is the equivalent resistance of the CA3080 ($R_{eq} = 23.7k$ when $I_{ABC} = 1\text{ ma}$). Consulting Fig. 5 on page 6 of this issue, we see that the center frequency of the filter is $1/2\pi R_{eq} C$. We saw above that the current into pin 5 of the CA3080's on page 16 was limited to about 0.83ma, corresponding to $R_{eq} = 28.6k$, and since $C = 330\text{pf}$, we get an upper frequency limit of about 17 kHz, corresponding well to the 18 kHz observed. We can also obtain from the information on Fig. 5 on page 6 that Q is equal to the inversion of the gain from the bandpass output back to the high-pass output. With the Q control in its minimum position (away from R23), the gain is $R16/R22 = 100k/27k = 3.7$ corresponding

to a Q of 0.27. With the Q control in its maximum position (toward R23), the gain is $(47/100k) \cdot (100k/27k) = 0.00174$ corresponding to a Q of 574. For higher Q, R23 may be set to 22 ohms with some possible loss of stability margin. The control voltage rejection pots are adjusted so that when the coarse frequency control is adjusted through its full range, the deflection at the low-pass output is a minimum. Set both at their midpoints to start with, then alternately adjust them until the deflection is a minimum. For non-critical work, you can just ground the (+) terminal of both 3080's and leave out TP-2, TP-3 and associated resistors R12-R15.

The phase lead circuitry was installed according to the general principles outlined above. We will describe here the exact method of determining the proper value for the compensation capacitor, and this will serve to indicate how the value should be set in other filters and for any exact testing by individual builders. The first step is to set a medium value of Q in the range of 5 to 50. It is not essential that the exact theoretical value for Q be known, but it is helpful to know this. In this circuit, we removed R22 and put a 1 meg resistor from the band-pass output to the (-) input of IC-2. This meant that the theoretical Q should have been 10. Next, the Q is measured as a function of frequency. At some frequency, it will be noted that Q has risen somewhat above the low frequency value (See Fig. 5). The Q at the highest frequency the filter will be used at should be noted. During testing, this was 25 kHz for the present filter. The rise of Q at higher frequencies is known as Q-enhancement. Once this enhancement is detected, it should be corrected. This is a matter of installing capacitors C3 and C4. We started with 18pf for these, and the values of Q were again measured. Note that this resulted in overcompensation since the Q comes down at higher frequencies. However, excellent stability was obtained with the 18pf value. We then tried 10pf for these capacitors and found it leveled off the Q quite well. In testing for higher values of Q, we found we could get values of Q up to 1000 at 10kHz with the 10pf capacitors. However, at times, such a high Q at 25 kHz resulted in instability. Rather than increase the values of C3 and C4, we thought it better to cut back the maximum frequency by increasing R35 and R36 to 18k.

Since Q is in the range of 5 to 50 for this case, a number of methods can be used to measure Q, and these can be found in the first report on bandpass filters in this newsletter. Note that the ringing method can be used even if a scope with an accurate time base is not available. All that is required is a VCO or other function generator that produces a sawtooth of fairly well known frequency. The setup is shown in Fig. 6. The sweep frequency is adjusted until the amplitude at the end of the trace on the scope is $1/e = 37\%$ of its starting value. Denoting this frequency by f_s , it is clear that the ring time of the filter is $1/f_s$, and $Q = \pi f_o T_{ring} = \pi f_o / f_s$ where f_o is the center frequency which has previously been determined by measurement with a sinewave input. Another useful method of leveling off the Q would be to control both the VCO and the VCF from the same voltage (assuming they track) as shown by the dotted line in Fig. 6. With this setup, the trace on the scope has a constant envelope if the Q is constant with frequency. If the end of the trace gets smaller as frequency goes up, less compensation is needed. If the end of the trace rises with frequency, more compensation is needed. This is probably one of the fastest ways of getting satisfactory leveling of Q. It might also be interesting to try a somewhat larger capacitor in the stage driven by the high-pass (C3) and a slightly smaller value for C4. The reason for this can be seen by consulting Fig. 3 where we see that the capacitor C3 compensates for two phase shifts while the capacitor C4 compensates for only one. However, it works well with both capacitors the same.

Finally, we decided to use an output mode switch because it will save some space on the panel, and otherwise we would need separate output buffers for each stage [the CA3140 is not satisfactory - see EN#69 (13)]. We thus use a buffer such as the type 556 since it is fast enough and is a satisfactory output driver. In any event, this additional op-amp would have been needed for a notch output. The inversion of IC-7 is also useful since a positive going transition on the input will cause the BP output to start to ring in the positive direction first, and this seems the most natural.

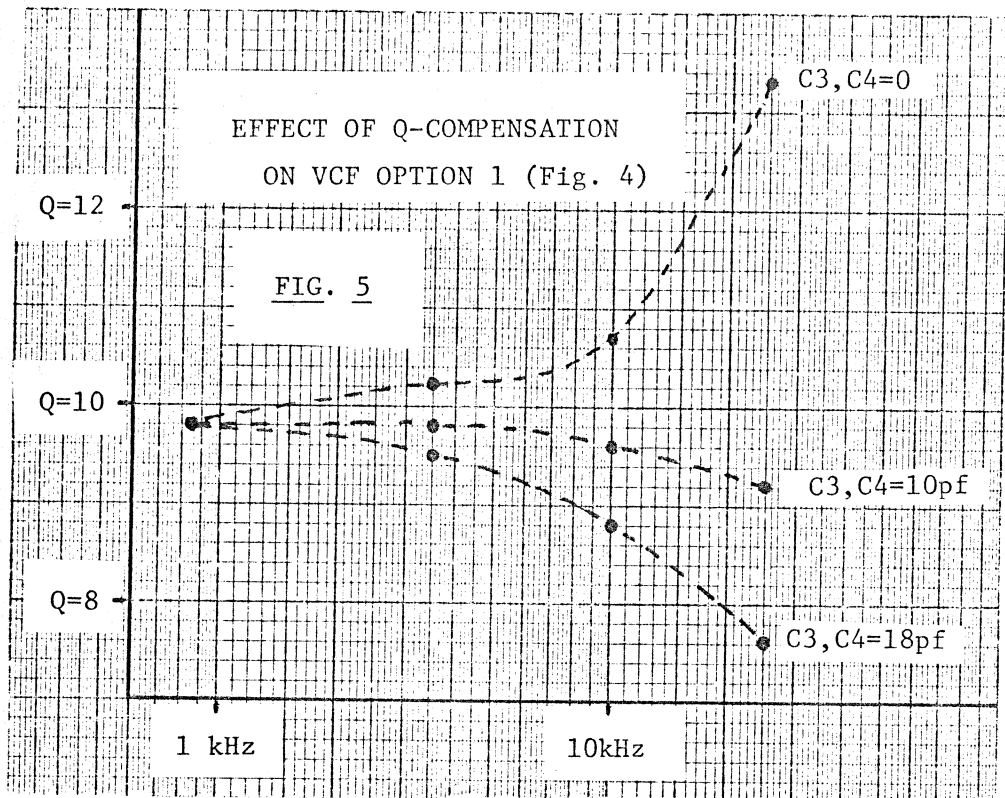
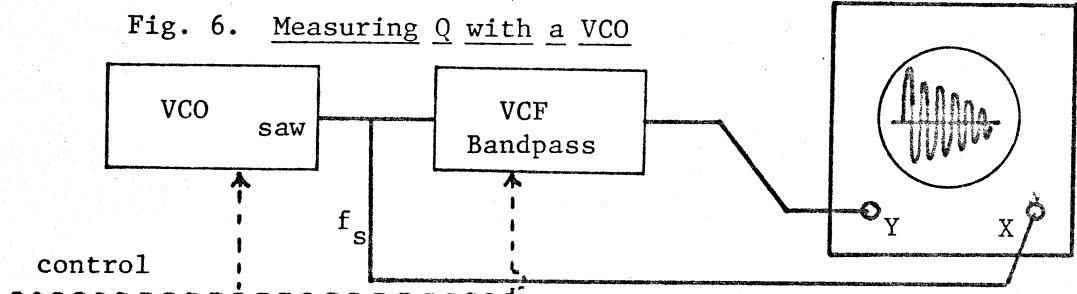


Fig. 6. Measuring Q with a VCO

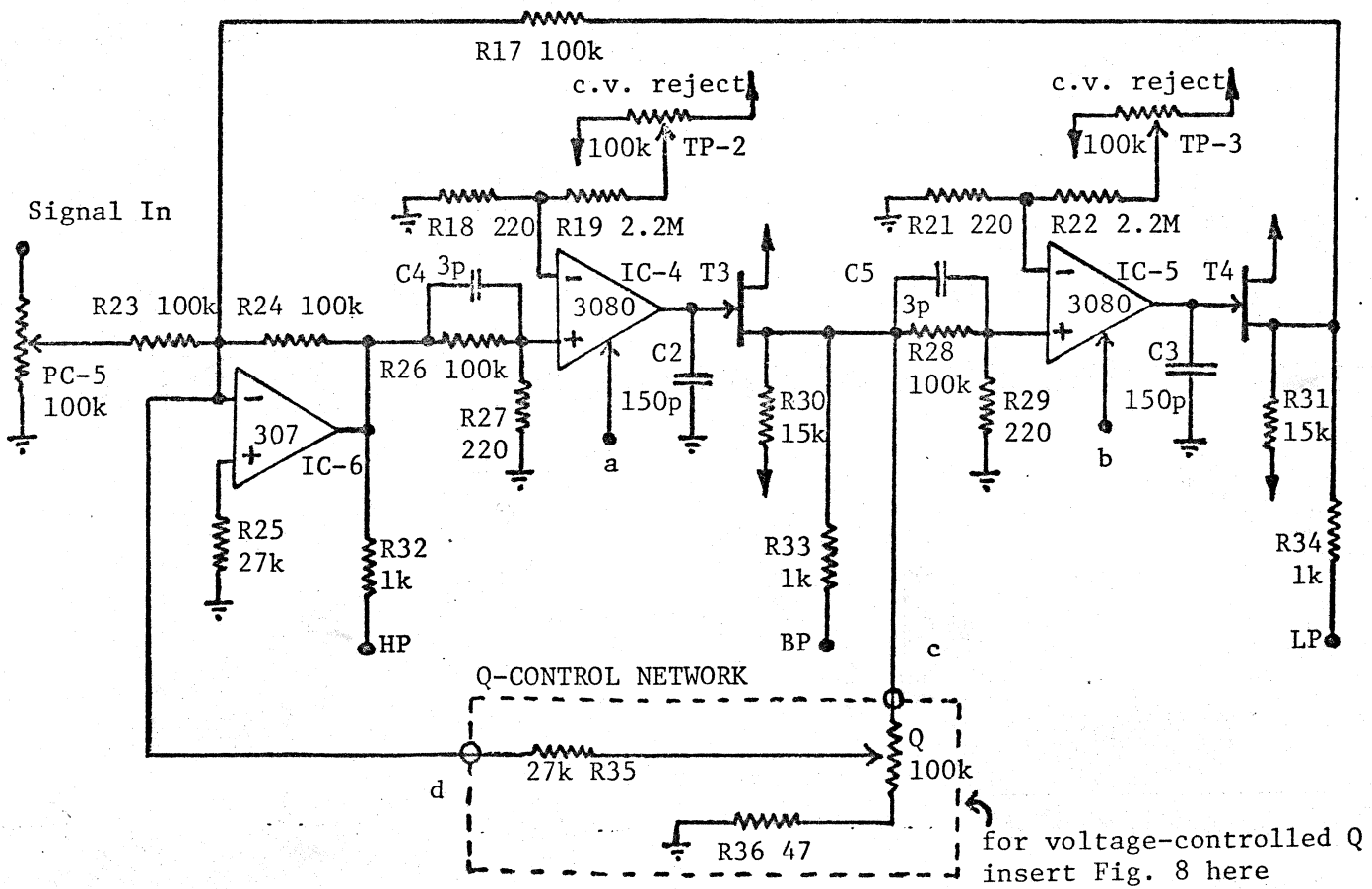
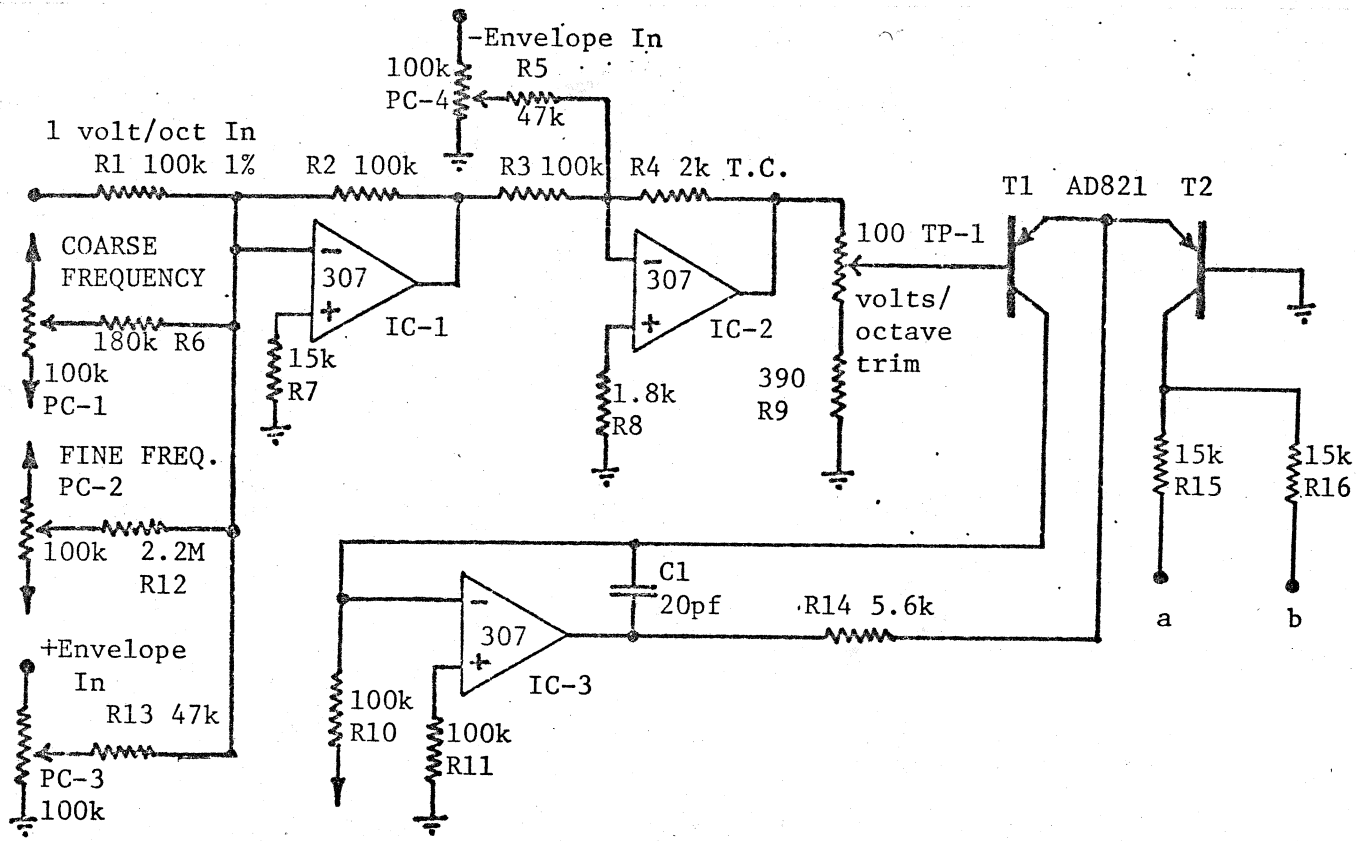


ENS-76 VOLTAGE-CONTROLLED FILTER - OPTION 2

The second option for the ENS-76 VCF is shown in Fig. 7 and Fig. 8. This filter is a modification of the EN#37 design. The exponential converter section of this filter uses a single current source split by two resistors (R15 and R16) to supply the two CA3080's. The exponential source from Option 1 could be used here. One advantage of the current source in Option 2 is that it has inputs for both positive and negative excursions of frequency in response to a positive going voltage. Also, if linear modulation of filter frequency should become as popular as linear FM in VCO's, this current stage can be given linear control by supplying additional current to IC-3's summing node.

The actual filter is similar to Option 1 except it uses FET buffers instead of op-amps, and has parallel outputs for all three filter functions, High-Pass, Band-Pass, and Low-Pass. We show in Fig. 7 a manual Q control network to keep the diagram simple, but the voltage-controlled Q section is shown in Fig. 8. This voltage-controlled Q section could also be used with Option 1. The voltage-controlled Q section is somewhat different from the EN#37 design. We use here cascaded inverting summers to sum the Q-control voltage (IC-6 and IC-7). T5 and T6 form an exponential current source that controls the CA3080, IC-8. When the control sum is zero (output of IC-7 is zero), the current into pin 5 of IC-8 is just $I_o = 15/R39 = 15/150k = 0.1ma$. The equivalent

FIG. 7 ENS-76 VCF OPTION 2



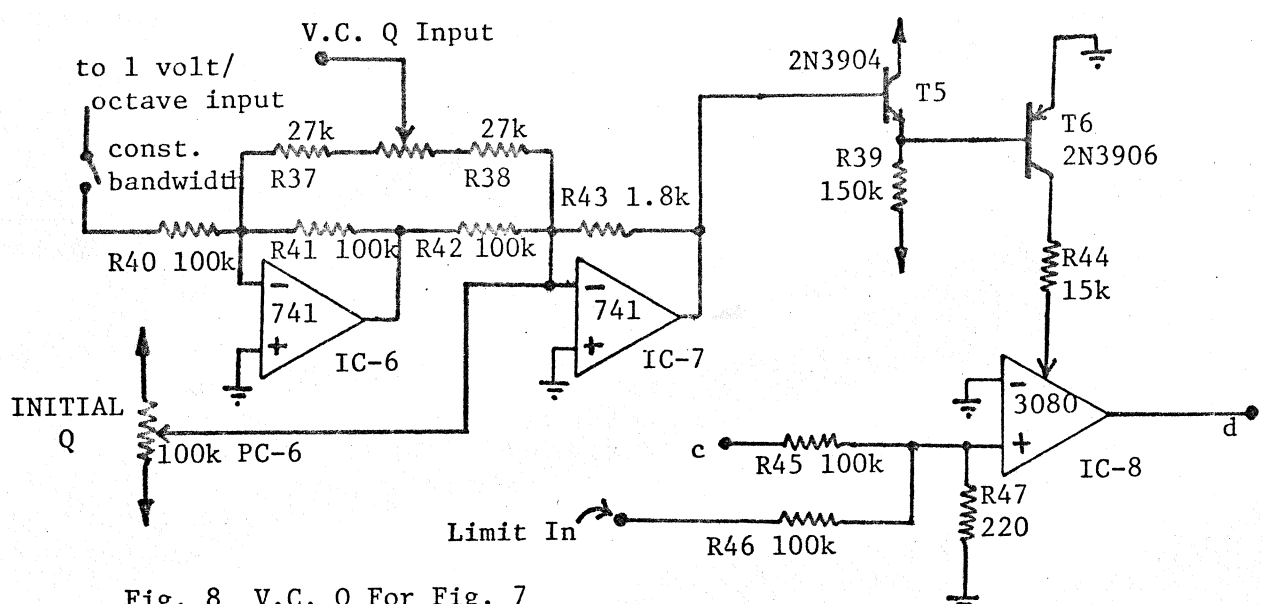
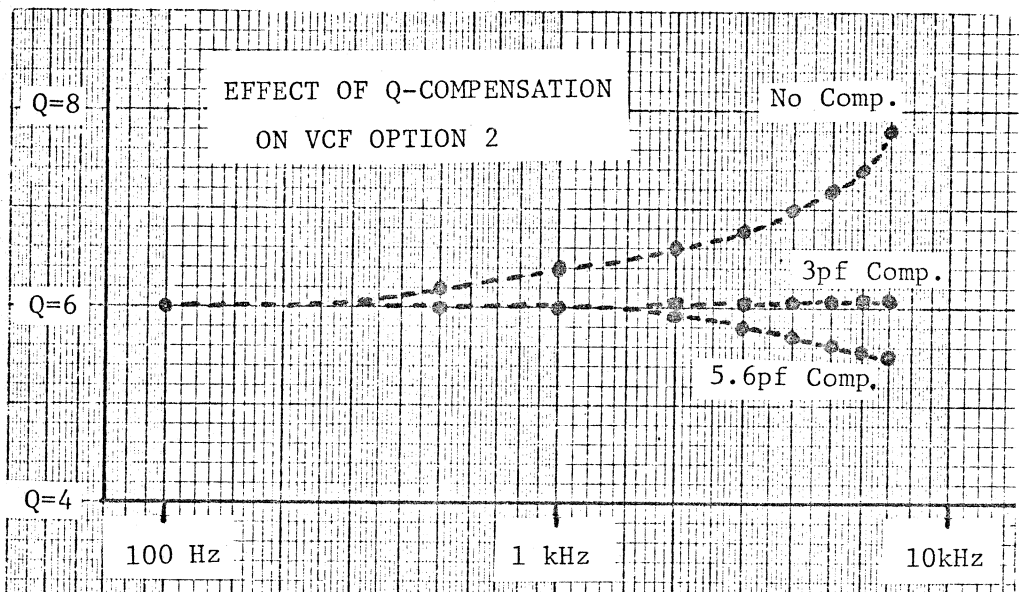


Fig. 8 V.C. Q For Fig. 7

Fig. 9



resistance of the CA3080 is thus $23.7/0.1\text{ma} = 237\text{k}$. Thus, the gain from BP back to HP is $100\text{k}/237\text{k} = 0.42$ corresponding to a Q of $1/0.42 = 2.4$ or so. Now, we provide a switch to connect R40 to the 1 volt/octave control voltage for the filter's frequency control section. A one volt change there will produce a 2:1 change of Q, and thus keep the bandwidth of the filter constant (resulting in a constant ring time independent of frequency). A variable v.c. Q input is provided as well. Note that to shut this one off the pot must be accurately centered, or the controlling source can be removed. The arrangement as shown will allow a unipolar envelope to either adjust the Q up or down depending on the setting of the V.C. Q Input control PC-7.

The filter is compensated for Q enhancement much as Option 1 was. The graph of Q and frequency as a function of the compensating capacitor is shown in Fig. 9. Note that while the optimum value (3pf) seems smaller than the 10pf used in Option 1, since the attenuating resistor is 100k in Option 2 while it was only 10k in Option 1, the 3pf here is equivalent to 30pf for a 10k attenuator. In fact, persons building this circuit new should make R26 and R28 10k, and R27 and R29 equal to 22 ohms, and then use about 30 pf to compensate for Q (thus 30pf for C4 and C5). It is easier to work with a value of 30pf than it is to work with 3pf since 3 pf is on the order of normal stray capacitances. The tests in Fig. 9 show the result with voltage-controlled Q, not with the manual Q.

* * * * *

RECORD REVIEWS: -by Craig Anderton (*Continued from EN#70*)

"DREAM WEAVER" by Gary Wright. This one is a commercial success, and much of that is due to electronics. Gary Wright has bubbled under the surface of recognition for several years, but he got a new lease on life after putting together his current band, which has no guitars---only keyboards, most of them synthesized, and a drummer. The extra novelty of sound (or whatever you want to call it) finally pushed him over the top. If anything, Mr. Wright is an over-achiever. The musical concepts are pleasant, but not earth-shattering; yet it seems clear that Mr. Wright believes in himself and his band, which makes it much easier to convince other people to believe in the music.

But there are limitations. The bass parts, being all synthesized, become repetitive and trite sounding very rapidly. Putting the bass sound through more modifiers could have helped, or some creative mixing could have made a world of difference. Having a conventional bass for just one or two cuts could also have broken the monotony. Additionally, the exclusive reliance on electronics produces a "thin" sound, as many electronic sounds are so simple structurally they can't sound complex. Whereas acoustic and many electric instruments have sympathetic resonances, varying attack and decay characteristics, and complex overtone structures, electronic devices have to make do with less. As such, the album does suffer from this.

I wouldn't say rush out and buy the album. But if a friend has it, give it a listen for a quick course in some of the strengths and weaknesses inherent in an all-electronic vehicle for what is essentially pop music.

"FIREBIRD" by Isao Tomita. There are some people who are avidly into rock music, like ELP or Yes, or Frank Zappa, who fail to realize the enormous debt these people owe to composers like Stravinsky, Cage, and Varese. Perhaps one reason for this is that many modern listeners can't make the transition from electronic implementation to acoustic instruments (how's that for a switch!), and lumps someone like Stravinsky in with Beethoven simply because the instrumentation is similar.

For these people, "Firebird" will be an educational experience. It preserves the feelings of Stravinsky, yes, but Tomita is not afraid to augment and interpret, which is good for us. Loud sounds are LOUD!!! and the attacks ATTack and the decays d e c a y, with all sounds presented as if under a magnifying glass. This album is great fun to listen to; a little heavy for your run-of-the-mill listening, perhaps, but then again "Firebird" is not exactly comedy. Tomita gets the sounds he wants from his equipment (and he has a lot of it).

One final comment: he avoids many of the flaws from his previous albums, such as overuse of the Mellotron. Patrick Moraz, take note.

CLASSIFIEDS:

FOR SALE: 1976 Signetics Data Manual (1200 pages) \$4.00; Analog Devices Nonlinear Circuits Handbook and Analog-Digital Conversion Handbook \$3.00 each; Cambion Thermoelectric Handbook \$1.00; 1975 American Microsystems Inc Guide to MOS Produces \$1.00; one-half-inch tape heads; 9-track, single gap per track; 7-track, separate read, write gaps per track, \$12 each. All orders/inquiries include SASE. Neil Benson, 8130 Pt Douglas Dr., Cottage Grove, NM 55016.
WANTED: Copy of Parametric Amplifiers by 73 Magazine. Neil Benson, 8130 Pt Douglas Dr., Cottage Grove, NM 55016 (612-372-7515 days).

WANTED: Source of mini 'transistor' size earphone jacks, closed or open circuit.
(212) 864-7414

ELECTRONOTES, Vol. 8, No. 71 [November 1976]

Published by B. A. Hutchins, 203 Snyder Hill Rd., Ithaca, NY 14850
Send Routine Orders to: ELECTRONOTES, 213 Dryden Rd., Ithaca, NY 14850 (607)-273-8030